

University of Texas Rio Grande Valley

ScholarWorks @ UTRGV

---

Mechanical Engineering Faculty Publications  
and Presentations

College of Engineering and Computer Science

---

11-3-2022

## Non-Destructive Infrared Thermographic Curing Analysis of Polymer Composites

Md Ashiqur Rahman

*The University of Texas Rio Grande Valley*

Javier Becerril

Dipannita Ghosh

*The University of Texas Rio Grande Valley*

Nazmul Islam

*The University of Texas Rio Grande Valley*, nazmul.islam@utrgv.edu

Follow this and additional works at: [https://scholarworks.utrgv.edu/me\\_fac](https://scholarworks.utrgv.edu/me_fac)



Part of the [Mechanical Engineering Commons](#)

---

### Recommended Citation

Rahman, Md Ashiqur, Javier Becerril, Dipannita Ghosh, and Nazmul Islam. 2022. "Non-Destructive Infrared Thermographic Curing Analysis of Polymer Composites." In Proceedings of the ASME 2022 International Mechanical Engineering Congress and Exposition. Columbus, OH: ASME.

This Article is brought to you for free and open access by the College of Engineering and Computer Science at ScholarWorks @ UTRGV. It has been accepted for inclusion in Mechanical Engineering Faculty Publications and Presentations by an authorized administrator of ScholarWorks @ UTRGV. For more information, please contact [justin.white@utrgv.edu](mailto:justin.white@utrgv.edu), [william.flores01@utrgv.edu](mailto:william.flores01@utrgv.edu).

## NON-DESTRUCTIVE INFRARED THERMOGRAPHIC CURING ANALYSIS OF POLYMER COMPOSITES

Md Ashiqur Rahman<sup>1</sup>, Javier Becerril<sup>1</sup>, Dipannita Ghosh<sup>1</sup>, Nazmul Islam<sup>1</sup>, Ali Ashraf<sup>1</sup>

<sup>1</sup>University of Texas Rio Grande Valley, TX, USA-78539.

### ABSTRACT

*Infrared (IR) thermography is a non-contact method of measuring temperature that analyzes the infrared radiation emitted by an object. Properties of polymer composites are heavily influenced by the filler material, filler size, and filler dispersion, and thus thermographic analysis can be a useful tool to determine the curing and filler dispersion. In this study, we investigated the curing mechanisms of polymer composites at the microscale by capturing real-time temperature using an IR Thermal Camera. Silicone polymers with fillers of Graphene, Graphite powder, Graphite flake, and Molybdenum disulfide (MoS<sub>2</sub>) were subsequently poured into a customized 3D printed mold for thermography. The nanocomposites were microscopically heated with a Nichrome resistance wire, and real-time surface temperatures were measured using different Softwares. This infrared thermal camera divides the target area into 640x480 pixels, allowing measurement and analysis of the sample with a resolution of 65 micrometers. Depending on the filler material, the temperature rises to a certain maximum point before curing, and once curing is complete, polymer composites exhibit a rapid temperature change indicating a transition from viscous fluid to solid. MoS<sub>2</sub>, Polydimethylsiloxane (PDMS) without filler, and PDMS with larger filler are ranked in order of maximum constant temperature. PDMS (without filler) cures in 500s, while PDMS-Graphene and PDMS Graphite Powder cure in about 800s. The curing time for PDMS Graphite flake is slightly longer (950s), while MoS<sub>2</sub> is around 520s. Therefore, this technique can indicate the influence of fillers on the curing of composites at the microscale, which is difficult to achieve by conventional methods such as differential scanning calorimetry. This nondestructive, low-cost, fast infrared thermography can be used to analyze the properties of polymer composites with different fillers and dispersion qualities in a variety of applications including precision additive manufacturing and quality control of curable composite inks.*

### 1. INTRODUCTION

Polymer composites, which are polymers reinforced with fillers of varying sizes, shapes, and weight fractions, have attracted the interest of researchers due to the unexpected synergistic properties obtained from the two components and their application in a variety of high-demand aerospace, wind energy, automotive, maritime or civil infrastructure, and consumer fields [1-6].

Because a variety of additives (e.g., promoting agents, fillers, etc.) are included in commercial formulations, resulting in complex cure kinetics, a thorough understanding of the curing process is the most significant precondition in composites process optimization [7]. Among all the curing methods for polymer composites, the most common is thermal curing. Additionally, different properties (viscosity, density, and thermal properties) of polymer composites, change during curing. During the curing phenomenon, the temperature rapidly changes due to phase transitions from liquid to solid. By measuring these temperature changes through an infrared thermal camera, we can analyze the properties (such as curing time, and dispersion) in a polymer composite. For example, this temperature change is greater with fillers than without fillers in photocured polymers [8]. Using a close-up lens infrared thermography, the dispersion, voids, and thermal characteristics of graphene polymer composites were investigated by Ashraf *et al.* [9]. Pantano *et. al* also investigated the poor dispersion of carbon nanotubes in nanocomposites using Infrared thermography [10]. The dispersion characterization of graphene nanocomposite was investigated using non-contact infrared thermography mapping, which evaluates the thermal diffusivity ( $\alpha$ ) and relates  $\alpha$  to a dispersion index [11]. Thus, the infrared thermography method can be utilized to monitor the curing phenomena of polymer composites to facilitate a quick and intriguing application when a uniform property is the main priority.

In this study, we investigated the curing phenomena of PDMS with different filler materials using non-destructive infrared thermography. As the constant current ( $i$ ) passes through a resistance ( $R$ ), it generates a constant heat rate equivalent to  $i^2R$  across the resistor. This heat was dissipated into the polymer composite samples in the chamber and different curing temperatures and corresponding curing times were found because of the different sizes and shapes of fillers in the composite materials. This non-destructive infrared thermography approach can be used to ensure uniform curing, and thus uniform mechanical and thermal properties at a higher spatial resolution, as well as to quantify filler dispersion and void in polymer composites.

## 2. MATERIALS AND METHODS

### 2.1 Materials

SYLGARD™ 184 Silicone Elastomer Kit was obtained from Dow Corning. Graphene nanoplatelets (surface area 750 m<sup>2</sup>/g, size ~2 μm) were acquired from Sigma Aldrich. Graphite powder was obtained from Fisher Chemicals. Graphite flake (size of ~270 μm), and Molybdenum Disulphide (MoS<sub>2</sub>-Powder size 1.5 μm) were provided by ACS Materials LLC.

### 2.2 Fabrication of Composites

PDMS with a curing agent (10:1) was taken in five different containers and then graphene, graphite powder, graphite flake, and MoS<sub>2</sub> were mixed in a 3% weight ratio (3% loading provided higher dispersion, we will study the effect of different loading percentages in future using a homogeneous shear mixer). Then, these polymer composites were poured into a customized 3D printed chamber (size of 4x3x2 mm<sup>3</sup>). Fluke RSE600 Thermal IR Camera with a close-up macro lens and an XYZ stage for focusing sample contained in the 3D chamber is shown in Fig. 1a-b. A nichrome wire (diameter of 127 micrometers) was then placed into the chamber, and the current (0.5 Amp) was passed by a Triple Output Programmable DC Power Supply BK Precision 9130B (Fig 1c). The IR Camera was used to measure the real-time temperature of a targeted region of the polymer composites in the 3D printed chamber. Temperature data was then analyzed via SmartView R&D, MATLAB Image Processing Tools, Excel, and Origin Pro software packages.

## 3. RESULTS AND DISCUSSION

Constant current through a resistive wire creates a heat rate equivalent to  $i^2R$ , and in this case, a nichrome wire was used to heat PDMS composites in a customized 3D printed chamber. PDMS cures after a certain time at a specific temperature. However, PDMS with fillers shows a different curing time than without fillers due to the interaction between filler and polymer. The constant heat flux supplied by the wire induced a different temperature profile due to heat capacity variation for different composites. As a consequence, the curing time for various composites varied due to this temperature variation. Furthermore, during curing, polymer composites experience a significant temperature fluctuation as curing generally involves

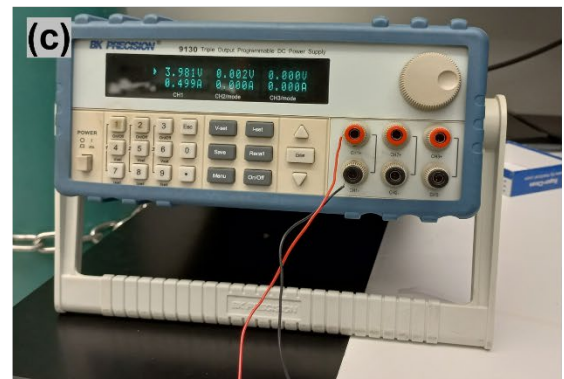
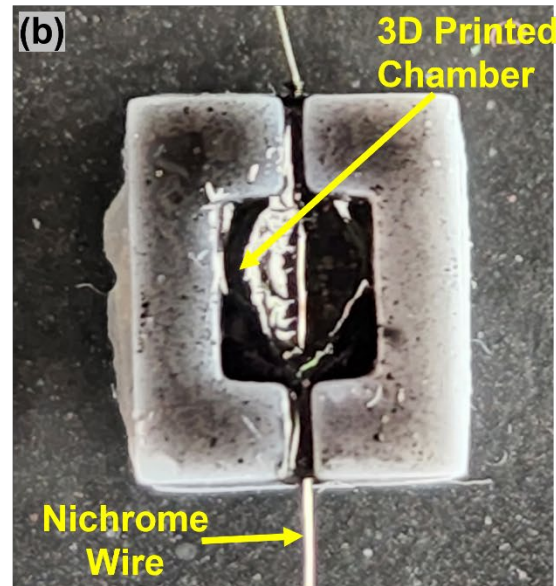
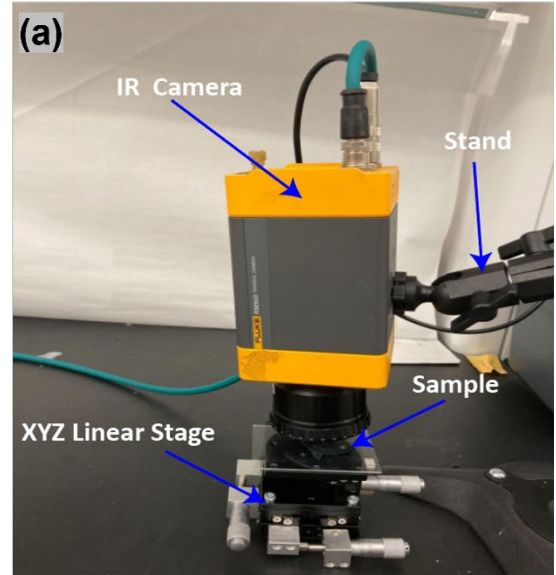


**Figure 1:** (a) Fluke RSE600 Thermal IR camera with XYZ stage, (b) Customized 3D printed chamber and nichrome wire connection setup, (c) BK Precision programmable DC power supply.

a phase change between liquid to solid. The total curing time and dispersion were calculated by measuring the real-time temperature with an infrared thermal camera and analyzing it with MATLAB Image Processing Tools.

The temperature profile at the center of the frame for PDMS, PDMS with Graphite powder, and PDMS with MoS<sub>2</sub> composites is shown in Fig. 2. Bare PDMS polymer reached a maximum temperature of ~150 (°C) at nearly 500 s, then after a slight temperature variation, it started increasing again. While for MoS<sub>2</sub> and Graphite powder, the temperature profiles were different as the heat capacity is different for the composites. PDMS MoS<sub>2</sub> reached a higher temperature (max. temperature ~160 °C) than bare PDMS as the heat capacity is higher in PDMS MoS<sub>2</sub> composite than PDMS. Conversely, for PDMS G powder, the temperature was always lower (max. temperature ~140 °C) than PDMS due to the lower heat capacity of the composite.

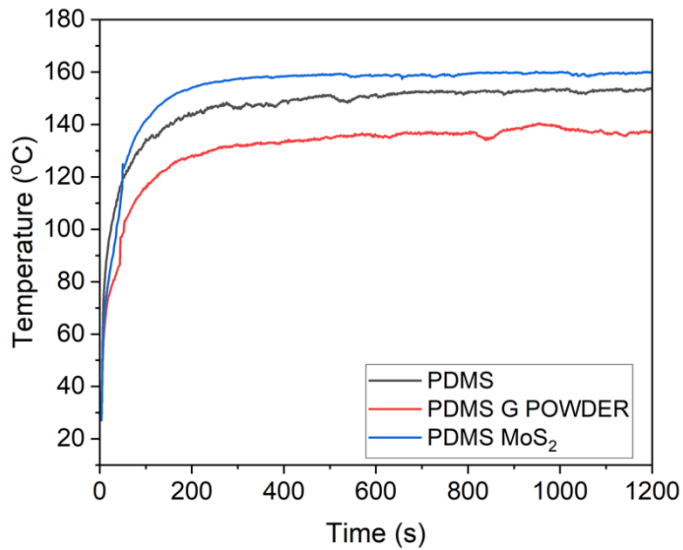


**Figure 2:** Temperature profile for PDMS, PDMS with Graphite powder, and PDMS with MoS<sub>2</sub>.

The temperature profile at the center of the frame of PDMS-Graphene, PDMS-Graphite powder, and PDMS-Graphite flake composites is shown in Fig. 3. As the size of the graphene is at the nanoscale, 3% weight percentage of graphene provided a homogenous mixing, and thus reached a temperature ~141 (°C) from room temperature. The temperature slightly went down and then jumped to ~143 (°C) at ~940 s and maintained the temperature afterward. As the size of Graphite powder and flake is higher than graphene, the temperature profile deviated from Graphene. For Graphite powder, the steady temperature reached ~136 (°C) ~800 s, suddenly dropped to 134 (°C), and then increased to a maximum value of 140 (°C). Similarly for Graphite flake, the temperature followed a similar profile at ~950 s but reached a lower temperature than Graphene and Graphite powder due to the lower heat capacity of composite. The reason behind graphite powder having different curing than the other

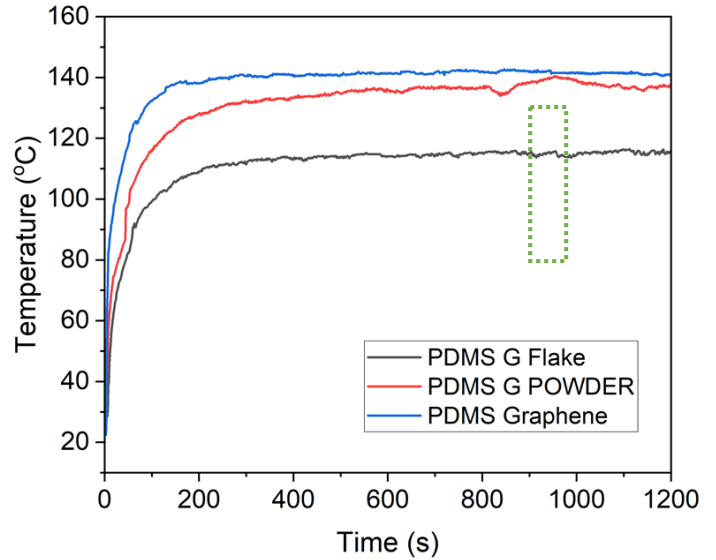


**Figure 3:** Temperature profile for PDMS with carbon material such as Graphite Flake (G flake), Graphite powder (G powder), and Graphene fillers.

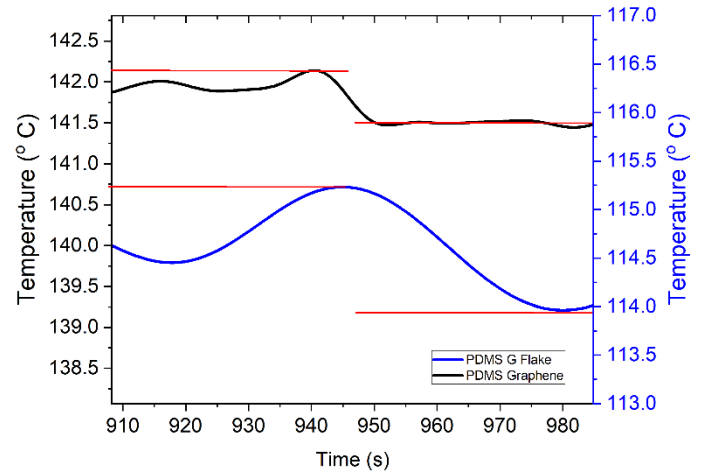


**Figure 4:** Temperature variation during curing for PDMS-Graphite flake and PDMS-Graphene (red horizontal line remarks peak temperatures). This is a magnified view of Figure 3 green dotted box.

two carbon filler composite samples are likely due to non-uniform dispersion, which we will investigate in future work.

For PDMS-Graphene composite, the temperature suddenly dropped from ~142.25 (°C) to 141.5 (°C) at time ~940s, while for PDMS Graphite flake temperature dropped down to 114 (°C) from 115.4 (°C) at similar time frame (Fig. 4). This sudden temperature change indicates curing and at this time, liquid polymer transforms into solids. Then the temperature again started increasing as the composite is fully cured to solid. From the temperature plot in Fig. 1 & 2, the curing time for PDMS, PDMS-MoS<sub>2</sub> and PDMS-Graphite powder were ~500 s, ~520 s,

and ~800 s respectively. This indicated the addition of filler delays curing and filler characteristics (material, size, and dispersion) will determine the lag in curing.

By analyzing different pixels from the infrared camera, we also characterized the curing phenomenon at different points or locations. In Fig. 5, PDMS with Graphite powder composites' four spatial locations were investigated. As the wire passed through the middle of the 3D chamber, the maximum temperature was higher in middle (point 3) than in any transverse direction (points 1 & 2) or longitudinal direction (point 4). The temperature profile for points 1, 3 & 4 was similar (~815 s) but point 2 was slightly different (due to inhomogeneity).

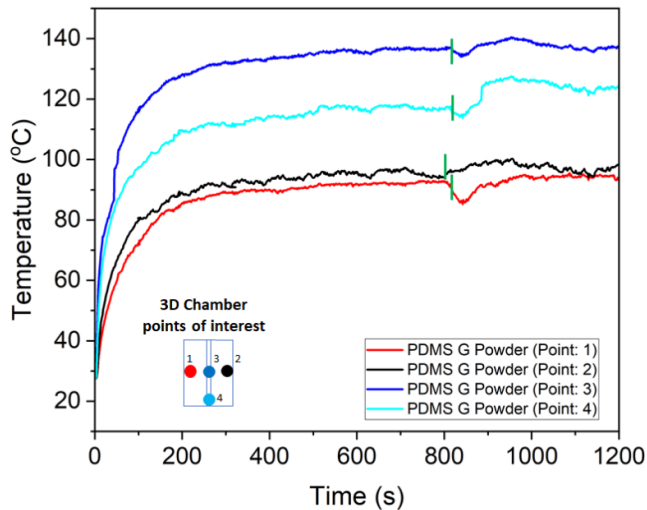


**Figure 5:** Temperature profile and curing time comparison for 4 different points of PDMS with graphite powder filler (green vertical line indicating the onset of curing).

Image processing tools from MATLAB were utilized to analyze the dispersion of graphite flake and MoS<sub>2</sub> in PDMS. Thermal images for PDMS with graphite flake obtained from the SmartView software are shown in Fig. 6. The nichrome was small in diameter (~0.127 mm), and the high heating zone was

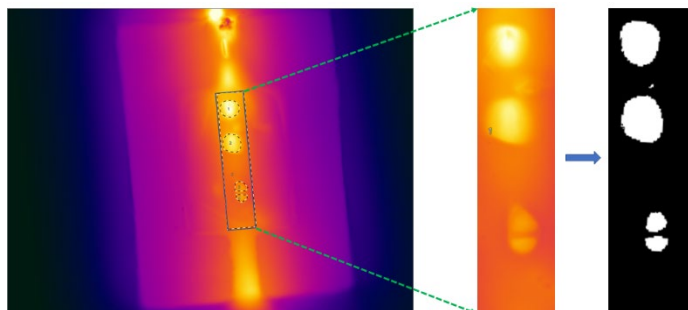


**Figure 6:** Thermal image of PDMS with graphite flake composite (left), heating zone with graphite flake in distinct color (middle), and the binary image obtained from image processing showing graphite flake in white color fill (right).

nearly a similar dimension in traverse direction (marked by a rectangle in Fig. 6 (left)). As the emissivity of the graphite flake was different from PDMS, the graphite flake was distinguishable in the thermal image. The heating zone area was then analyzed via image processing tools, and from the binary image it was proven that graphite flake was dispersed randomly (Fig. 6-right). Thus, the surface dispersion was calculated by using the following formula (equation 1):

$$\text{Surface Dispersion} = A_{\text{flake}}/A_{\text{total}} \quad \dots\dots\dots (1)$$

A<sub>flake</sub> is the pixel area of all flakes in the targeted region and A<sub>total</sub> is the total targeted area. So, the surface dispersion obtained was about ~18% for graphite flake (higher than the original loading, indicating a higher filler concentration near the surface).

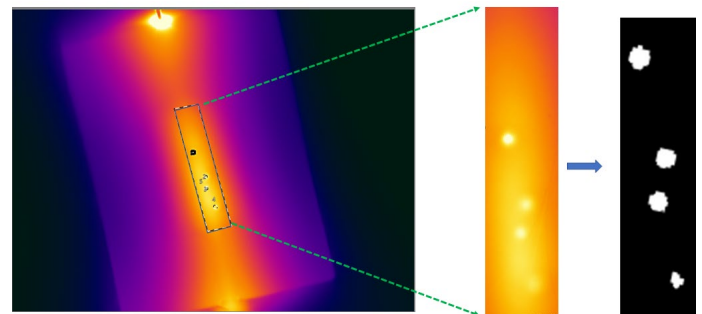


**Figure 7:** Thermal image of PDMS with MoS<sub>2</sub> composite (left), heating zone with MoS<sub>2</sub> in distinct color (middle), and the binary image obtained from image processing showing graphite flake in white color fill (right).

Similar to graphite flake, the thermal image, heating zone image, and binary image of PDMS with MoS<sub>2</sub> composite were shown in Fig. 7. Surface dispersion for PDMS-MoS<sub>2</sub> was ~2% by using the above-mentioned equation (similar to original loading, indicating better dispersion for small size MoS<sub>2</sub> fillers).

#### 4. CONCLUSION

Non-destructive infrared thermography is a useful tool to analyze the curing temperature and dispersion of different polymer composites. In this study, we investigated the curing phenomena of PDMS with varying sizes and shapes of graphene, graphite flake and powder, and MoS<sub>2</sub>. For constant heating, the curing time for PDMS was found to be dependent on filler type, size, and dispersion. A new formula was also proposed to determine the surface dispersion of graphite flake and MoS<sub>2</sub>. In aerospace or industrial applications where uniform dispersion of polymer composites is required, infrared microscale thermography can be an effective method for analyzing both curing and surface distribution of filler materials.

#### ACKNOWLEDGEMENTS

This research is financially supported by National Science Foundation (NSF) under grant number ERI 2138574. We acknowledge the suggestions provided by Mr. Md Imrul Kaish



from the Department of Electrical Engineering at The University of Texas Rio Grande Valley. We also thank Fluke Corporation for providing us the software support.

## REFERENCES

- [1] Irving, P. E., and Soutis, C., 2019, *Polymer composites in the aerospace industry*, Woodhead Publishing.
- [2] Hayman, B., Wedel-Heinen, J., and Brøndsted, P., 2008, "Materials challenges in present and future wind energy," *MRS bulletin*, 33(4), pp. 343-353.
- [3] Volpe, V., Lanzillo, S., Affinita, G., Villacci, B., Macchiarolo, I., and Pantani, R., 2019, "Lightweight high-performance polymer composite for automotive applications," *Polymers*, 11(2), p. 326.
- [4] Tran, P., Nguyen, Q. T., and Lau, K., 2018, "Fire performance of polymer-based composites for maritime infrastructure," *Composites Part B: Engineering*, 155, pp. 31-48.
- [5] Hollaway, L., 2003, "The evolution of and the way forward for advanced polymer composites in the civil infrastructure," *Construction and Building Materials*, 17(6-7), pp. 365-378.
- [6] Hollaway, L. C., 2001, *Advanced polymer composites and polymers in the civil infrastructure*, Elsevier.
- [7] Yousefi, A., Lafleur, P., and Gauvin, R., 1997, "Kinetic studies of thermoset cure reactions: a review," *Polymer Composites*, 18(2), pp. 157-168.
- [8] Alabdali, Z. N., Irizarry, E., Reiter, M. P., Ashraf, A., Lynch-Branzoi, J. K., and Mann, A. B., 2021, "Low-weight fractions of graphene and hydroxyapatite enhance mechanics in photocured methacrylate adhesives," *Journal of Applied Polymer Science*, 138(20), p. 50442.
- [9] Ashraf, A., Jani, N., Farmer, F., and Lynch-Branzoi, J. K., 2020, "Non-destructive investigation of dispersion, bonding, and thermal properties of emerging polymer nanocomposites using close-up lens assisted infrared thermography," *MRS Advances*, 5(14-15), pp. 735-742.
- [10] Pantano, A., Montinaro, N., Cerniglia, D., Micciulla, F., Bistarelli, S., Cataldo, A., and Bellucci, S., 2019, "Novel non-destructive evaluation technique for the detection of poor dispersion of carbon nanotubes in nanocomposites," *Composites Part B: Engineering*, 163, pp. 52-58.
- [11] Gresil, M., Wang, Z., Poutrel, Q.-A., and Soutis, C., 2017, "Thermal diffusivity mapping of graphene based polymer nanocomposites," *Scientific reports*, 7(1), pp. 1-10.